

## CHARACTERIZING FOULING TENDENCY OF CRUDE OIL ON A SURFACE USING A HIGH TEMPERATURE VARIABLE SHEAR COUPON TEST RIG

**P. Singh<sup>1</sup>, \*S. Krishnaswamy<sup>1</sup>, K. Ponnani<sup>2</sup>, A. Verma<sup>3</sup> and J. Rawat<sup>3</sup>**

<sup>1</sup>Centre of Excellence in Process Engineering & Intensification (COE-PE&I),  
Department of Chemical Engineering, BITS-Pilani K K Birla Goa Campus, Goa, India

\*E-mail address: [srinivas@goa.bits-pilani.ac.in](mailto:srinivas@goa.bits-pilani.ac.in)

<sup>2</sup>15/151 (old 7/383) Sreenivas, Sivan Kovil Street, Tharakkad, Palakkad, Kerala-678001, India

<sup>3</sup>Bharat Petroleum Corporation Limited, Corporate R & D Center, Greater Noida, India

### ABSTRACT

The present study experimentally demonstrates the ability of a High Temperature Variable Shear (HTVS) coupon test rig to characterize fouling under dynamic flow conditions. Experiments were conducted in a 2-litre batch autoclave system with provision to immerse metal coupons into the stream. Experiments were conducted covering bulk temperatures and stirrer speeds (which incorporated a shear effect) ranging from 250 °C to 300 °C and 100 to 600 RPM respectively. Parts of the foulant deposits collected were found to strongly (hard) and weakly (soft) adhere to a coupon surface. These deposits were subsequently characterized independently using Thermogravimetry (TGA), Elemental analysis, Scanning Electron Microscopy (SEM) and X-Ray Diffraction (XRD). The nature of soft deposits was found to be distinct from the nature of crude oil used. Corrosion was found to be the dominant fouling mechanism in this work. The results obtained confirm the potential of this test rig in understanding fouling tendency of liquid refinery streams on a surface.

### INTRODUCTION

Petroleum refining has long been the primary backbone for meeting global energy demands, producing fuels that have been used in industry, transportation and homes. Fouling from light and heavy crude oil streams during processing has been identified as a major cause of suboptimal operation in refinery systems resulting in plant downtime and production loss [1], [2]. Several studies have been carried out over the years to better understand the complex mechanisms associated with fouling in refinery equipment ranging from molecular to lab and plant scale. Several of these studies were mainly concerned with examining the impact of fouling on heat transfer, particularly on tubular test surfaces [3]–[6]. Attempts have also been made to characterize foulant deposits in some of these

studies [3], [7]–[15]. Heat transfer investigations and deposit characterization in several of these studies has been based on the flow of multiple streams over surfaces under varying operating conditions. A deeper insight into refinery fouling can be obtained by testing an individual stream under a specific operating condition of interest. This formed the genesis of the present work.

This study demonstrates the potential of a High Temperature Variable Shear (HTVS) coupon test rig in understanding fouling due to sulfidic corrosion over a wide range of temperature and rotational speeds. A custom design setup was built for this purpose. The use of HTVS was earlier demonstrated for a limited temperature range at a fixed rotational speed by Singh et al. [18]. The setup design was based on an approach adopted by Wang and Watkinson [11], [16], [17] who studied fouling on a cylindrical surface immersed in a rotating fluid at temperatures greater than 350 °C. The rig facilitates easy removal of deposits for further analysis and characterization. Details of the rig, experiments performed and results are reported herewith. The temperature range covered in this study corresponds to that prevalent in the crude Pre-Heat Exchanger Train (PHT) in a refinery. The effect of rotational speed not included in [18] is also reported.

### EXPERIMENTAL SETUP AND PROCEDURE

Fouling experiments were carried out in a custom-made test rig comprising of a 2-liter stainless steel autoclave (120 mm ID and 300 mm height) surrounded by a 2.5 kW ceramic band heater fitted with a controller. A schematic of the autoclave internals is shown in Fig. 1. The controller was driven by a temperature sensor that measured the outer surface temperature of the autoclave. This facilitated maintaining the fluid temperature at a desired value during the test runs. The autoclave and heater assembly were insulated using glass wool. A head assembly enabled closing of the system when

in operation. A photograph of the test unit is shown in Fig. 2.

Pressure was measured using a Bourdon pressure gauge (WIKA make, range: 0 – 100 bar, accuracy:  $\pm 1.0\%$  of full scale) and also using a WIKA make pressure transmitter (range: 0 – 150 bar, accuracy:  $\pm 0.5\%$  of full scale). A reflux condenser was used to condense any low boiling vapors arising from the sample which were directed

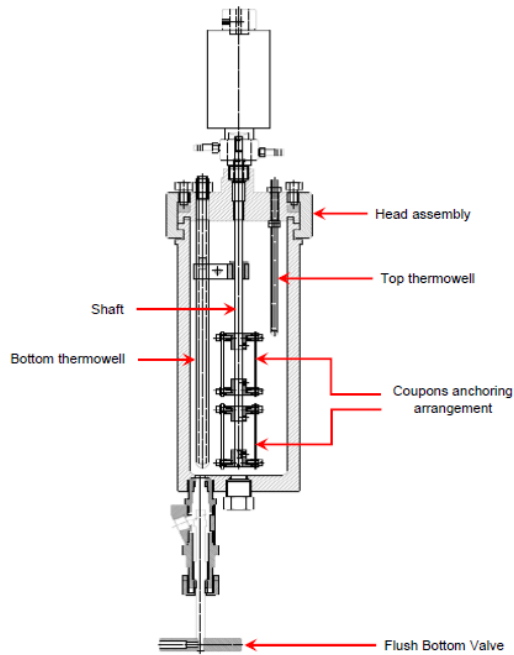


Fig. 1. Schematic of autoclave internals.

back into the autoclave by gravity. A vent valve at the condenser outlet was used to depressurize the system at the end of every run. The fluid temperature was measured using two Nickel-chromium/Nickel-aluminum (K type) thermocouples positioned at a distance of 135 mm and 290 mm from the head assembly. Samples were discarded after each run using a Flush Bottom Valve.

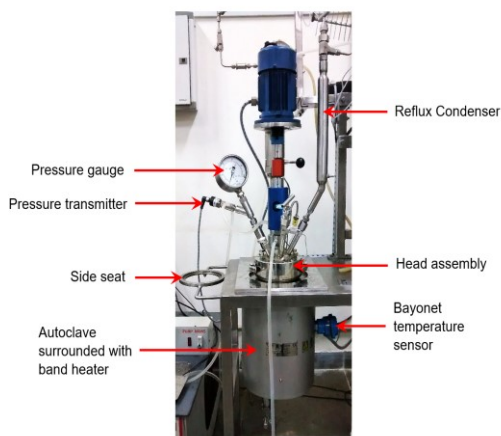


Fig. 2. Photograph of coupon test rig (Reproduced from [18])

Carbon steel (AISI 1060) coupons with dimensions of 7.5 cm (length)  $\times$  1.2 cm (width)  $\times$  0.1 cm (thickness) were used for experimentation. These coupons were fixed vertically at two prescribed levels on a solid central shaft which could be rotated up to 1450 RPM. A maximum of 6 numbers of coupon (at 60° positions on a discs) could be anchored at a particular level. Fig. 3 shows the photograph of a test coupon. A SCADA based Data Acquisition System (AMAR DAS 4.0) provided by Amar Equipment Pvt. Ltd. (Mumbai, India) was used to record data.

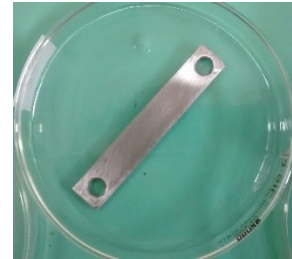


Fig. 3. Test coupon.

The experimental procedure was initiated by measuring the coupon surface roughness using a surface roughness tester (Surfrest SJ-410 Series Mitutoyo make, Japan). Before measurements, the coupons were polished with emery paper of 180 grit to eliminate surface flaws if any. The coupons were then independently weighed and anchored to the shaft. The autoclave was filled with the 1.8 liters of test fluid and closed. The system was pressurized to 30 bar (g) with nitrogen and leak tested for 2 hours. The system was then depressurized to  $\sim 8$  bar (g). The nitrogen purging also ensured removal of air from the vapour space of the autoclave.

The fluid was first heated to attain a desired bulk temperature at a prescribed RPM. Tests showed that no significant deposition occurred during this heating process. The system was allowed to operate for 80 hours following which the heater was switched off. The system was then cooled and depressurized. The head assembly along with coupons attached to the shaft was removed and kept on a side seat (see Fig. 2) for 8 hours. This ensured gravity draining and removal of any excess amount of the test fluid which would have adhered to the coupons during experimentation.

Each coupon with accumulated foulant deposits was detached from the shaft, washed using 100 ml of n-heptane, dried for 1 hour at room temperature and weighed. Deposits washed away with n-heptane were collected in a petri dish. The petri dish and its contents were weighed after evaporating the solvent in an oven for 8 hours.

## RESULTS AND DISCUSSIONS

A crude oil sample provided by BPCL Corporate R&D Centre was used for

experimentation. The important properties of the oil are listed in Table 1.

**Table 1** Properties of crude oil<sup>#</sup>

Element	Result
API	30.87
Viscosity (cP) @ 38 °C	2.631
Viscosity (cP) @ 200 °C	0.843
C (wt. %)	84.22
H (wt. %)	12.13
N (wt. %)	1.33
S (wt. %)	1.83
Saturates (wt. %)	25.58
Aromatics (wt. %)	44.38
Resins (wt. %)	27.37
C <sub>7</sub> -Asphaltenes* (wt. %)	1.76
CII	0.38
Fe (ppm)**	2.31
Mg (ppm)**	1.26
Na (ppm)**	7.16
Ni (ppm)**	6.95
Si (ppm)**	86.54
V (ppm)**	17.7

<sup>#</sup> Reproduced from [18]; \*Estimated using ASTM D 6560 protocol. \*\*Elemental analysis done using ICP – AES.

Foulant deposit was collected from each coupon post washing with n-heptane. A part of the deposit formed was carried away by n-heptane, while a portion remained strongly adhered to the coupon surface and could only be removed by scraping. These are henceforth referred to as soft and hard deposits respectively.

In the subsequent sections, influence of bulk temperature and rotational velocity on the amount of hard and soft deposit formed on a coupon surface is discussed.

#### Effect of bulk temperature

The impact of fluid bulk temperature at 100 RPM on the amount of hard and soft deposit is shown in Fig. 4 at 250, 275 and 300 °C. The results presented are for a single representative coupon (C1) immersed in the test fluid during the above runs. The average coupon surface roughness ( $R_a$ ) across these three runs was 1.584  $\mu\text{m}$ . The variation in coupon surface roughness between 250 and 300 °C was 0.059  $\mu\text{m}$ .

The amount of hard and soft deposit formed on the coupon surface increases with temperature. At 250 °C, the soft deposit is one order of magnitude higher in amount than the hard deposit. The orders are comparable at 275 and 300 °C due to increase in the rate of FeS formation (via a corrosion mechanism) at these temperatures. The FeS formed is part of the hard deposit (confirmed later by characterization). Sulfidic corrosion based fouling on carbon steel has been reported as a predominant mechanism in past works at 260 °C and above with

the corrosion rate increasing above this temperature [16], [17].

The higher temperature also promotes chemical reactions among organic species in the soft deposit. These reaction rates dominate the rate of formation of FeS at higher temperatures (> 275 °C). These soft deposits will subsequently adhere to the FeS layer due to change in surface characteristics. This will result in a higher organic content in hard deposit (as confirmed by TGA).

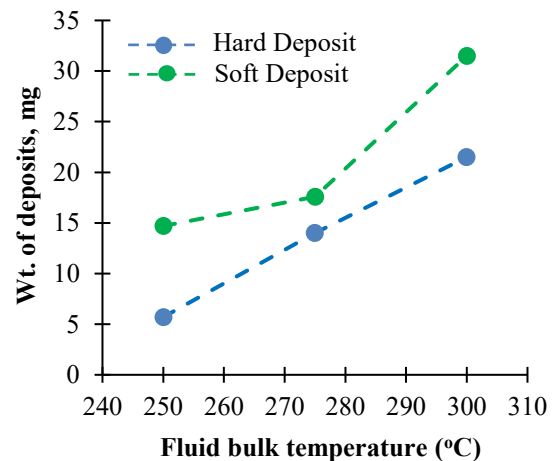


Fig. 4. Effect of bulk temperature on formation of hard and soft deposits at 100 RPM after 80 hours

The effect of temperature on hard and soft deposits was also investigated at 250 RPM and is shown in Fig. 5.

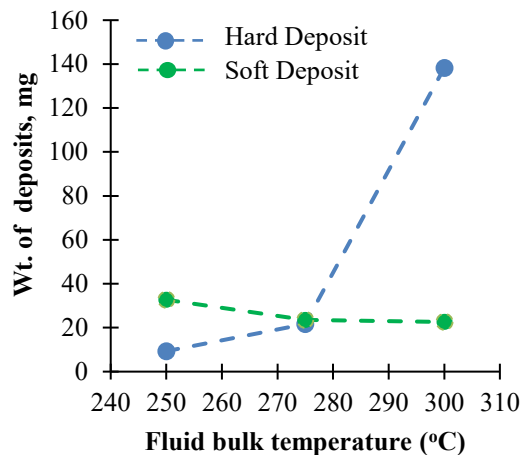


Fig. 5. Effect of bulk temperature on formation of hard and soft deposits at 250 RPM after 80 hours.

The trend in hard deposit was found to be similar. However, a significant increase in amount of hard deposit was observed beyond 275 °C. This is due to the increased attachment of organic content in soft deposit to the FeS layer formed. At these temperatures, the attachment is also preceded by increased rate of chemical reactions of FeS

formation and chemical species in the soft deposit. The soft deposit is found to decrease with increase in temperature.

### Effect of RPM

The effect of RPM at a constant temperature on the amount of hard deposit formed on a coupon surface after 80 hours is shown in Fig. 6. The results are presented for 2 representative coupons (C1 and C2). Apart from 100 RPM at 275 °C, test runs were also conducted at 250, 400 and 600 RPM without changing the bulk temperature. The range of shear stress and Reynolds number ( $Re$ ) corresponding to these RPM values is 0.18 to 3.88 Pa and ~2100 to ~16000 respectively. The shear stress was estimated using the correlation [17], [19]

$$\tau_c = 0.079 \times Re_c^{-0.3} \times \rho \times u_c^2 \quad (1)$$

The coupon Reynolds number was calculated using

$$Re_c = \frac{\Omega R_c L}{\nu} \quad (2)$$

The angular velocity was calculated from

$$\Omega = \frac{2\pi N}{60} \quad (3)$$

The amount of hard deposit is initially found to increase with rotational velocity (till 400 RPM) and subsequently decreases. The consistency in the trend obtained was confirmed using another Coupon (C2).

At a given bulk temperature, an increase in RPM promotes increased mixing of the fluid resulting in more foulant precursors or foulant being transported from the bulk to the coupon surface by advection / diffusion. However, the higher RPM will also promote removal rate of deposit from the vicinity of the coupon surface. This can be attributed to the increase in shear stress at the coupon surface when new and later at the deposit fluid-interphase. As the RPM increases the corresponding shear stress increase will reduce contact or residence time for deposit adhesion to occur on the surface [1]. The trends obtained in Fig. 6 can be due to the competing effects of transport and adhesion with the former dominating over the shear stress at RPM below 400. Such a trend where the fouling rate goes to a maximum has been reported in earlier work [17], [20].

The effect of RPM on soft deposit formed was also investigated and is shown in Fig. 7. Both coupons show similar trends from 250 RPM (corresponding shear stress: 0.88 Pa) onwards. The trend in soft deposit also exhibits a maxima at 400 RPM (corresponding shear stress: 1.95 Pa) due to the dominating effect of transport over shear. The rate of decrease in amount of soft deposit beyond 400 RPM is relatively lower as compared to the rate

of decrease in amount of hard deposit. The discrepancy in soft deposit values for the two coupons at a shear stress of 0.18 Pa can be attributed to flow conditions being laminar and applicability of equation 1 in this flow regime.

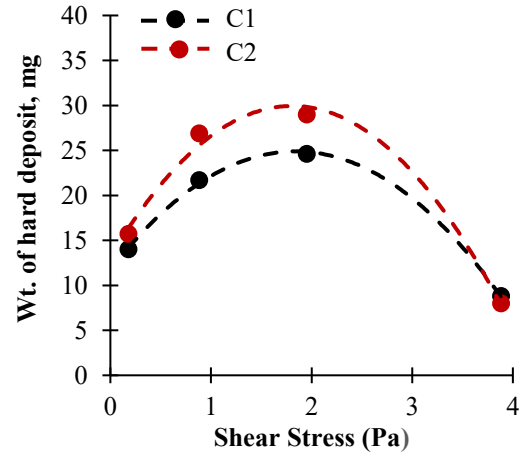


Fig. 6. Effect of shear stress on formation of hard deposit at 275 °C after 80 hours

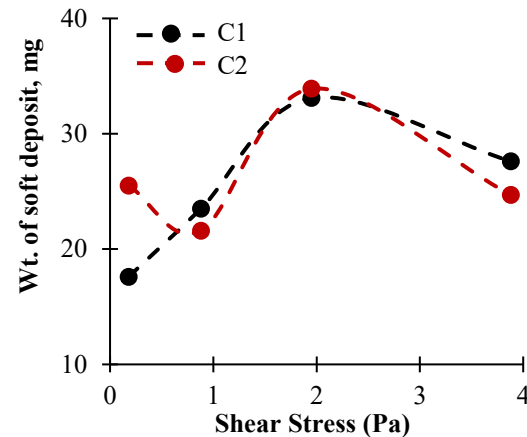


Fig. 7. Effect of shear stress on formation of soft deposit at 275 °C after 80 hours.

### Characterization of hard deposit

Hard deposits were collected after 80 hours from test runs carried out at 275 °C at 100 and 250 RPM. These deposits were scraped from both surfaces of a single coupon using a stainless-steel scalpel and cumulatively collected from 8 coupons. The deposits were characterized using TGA, CHNS and XRD. The TGA (Make: TA Instruments (Waters), Model: Discovery SDT 650) was used to determine volatile, combustible and ash content in the sample, the weight percentage of which is given in Table 2. At 275 °C, the deposit is inorganic in nature with a high ash content (>75%).

The TGA results for hard deposits collected at 300 °C and 250 RPM is shown in Table 3. The organic material content is found to increase with

temperature. The increase in volatile fraction is relatively higher as compared to the increase in combustible fraction. The organic content is likely to originate from the soft deposit.

**Table 2** TGA result of hard deposit at fixed temperature and varying RPM

Components	Hard deposit composition (wt. %)	
	275 °C, 100 RPM*	275 °C, 250 RPM
Volatiles	8.4	13.03
Combustibles	7.3	11.42
Ash	84.3	75.55

\*reproduced from [18]; shown for comparative purposes

**Table 3** TGA result of hard deposit at fixed RPM and varying temperature

Components	Hard deposit composition (wt. %)
	250 RPM, 300 °C
Volatiles	25.45
Combustibles	14.50
Ash	60.00

The sulfur content in the deposits was estimated using a CHNSO analyzer (Make: Perkin Elmer, U.S.A, Model: 2400 Series II). This analysis also helped quantify the content of Carbon (C), Hydrogen (H), and Nitrogen (N) in the deposits. The results are tabulated in Table 4.

The results confirm a relatively high content of sulfur in the deposit samples. The hydrogen to carbon (H/C) ratio was found to be 1.73 and 1.10 at 100 and 250 RPM respectively. These H/C values are indicative of the fact that the organic content in the deposit at the two temperatures investigated has degraded less with time to form coke-like material. The sulfur content at 300 °C at the two RPMs' was 29.77 and 26.02 respectively.

**Table 4** CHNS analysis data for hard deposit

Elements	Composition (wt. %) (275 °C, 100 RPM)*	Composition (wt. %) (275 °C, 250 RPM)
C	7.84	10.53
H	1.13	0.97
N	0.01	0.07
S	32.34	32.97

\*reproduced from [18]; shown for comparative purposes

The XRD spectra of a hard deposit sample at 275 °C and 250 RPM is shown in Fig. 8. The analysis was carried out for 2 $\theta$  values from 10 to 80° using an X-Ray Diffractometer (Model: Bruker D8 Advance). The spectra show characteristic peaks of iron sulphide and iron oxide. The peak intensities confirm the deposit samples to mainly contain FeS

as compared to FeO. Similar spectra were obtained for hard deposit samples collected at other temperatures and RPMs'.

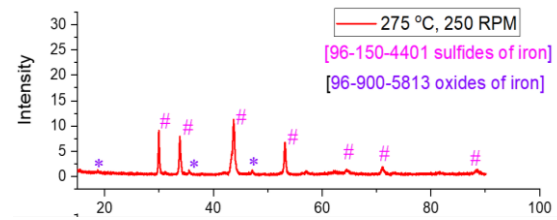


Fig. 8. XRD spectra of hard deposit at 275 °C and 250 RPM

### Surface morphology of coupon surface

Fig. 9 shows the morphology of a coupon surface with hard deposit at 275 °C and 100 RPM. The micrograph indicates agglomeration of deposit structures on the coupon.

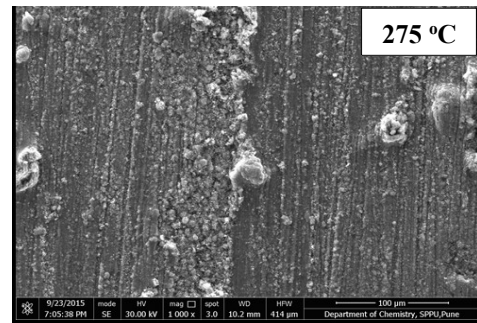


Fig. 9. SEM image of coupon surface with deposit at 275 °C and 100 RPM

Elemental mapping of hard deposits on a coupon surface at 300 °C and 100 RPM is shown in Fig. 10. The presence of sulfur at this temperature was consistent with the XRD spectra obtained for this element at the same temperature reported in [16].

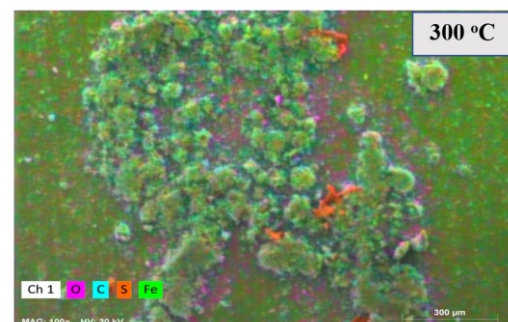


Fig. 10. Elemental mapping on coupon surface with hard deposit at 300 °C, 100 RPM (Reproduced from [16])

### Characterization of soft deposit

Soft deposit collected at 275 °C and 250 RPM was analyzed using a TGA and found to be largely organic in nature. The composition of volatiles and combustibles was more than 95%. Past works have reported this part of the deposit to contain trapped crude oil [4]. Subsequently, a TGA analysis of fresh and used crude oil was carried out. Fig. 11 shows the thermal behavior of soft deposits collected along with that of the crude samples taken before and after the test run at 275 °C.

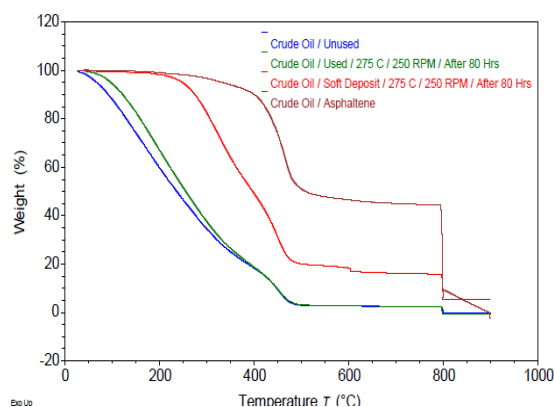


Fig. 11. Thermal analysis of crude oil, soft deposit and C<sub>7</sub> asphaltenes at 275 °C, 250 RPM

The figure also includes the thermal history of C<sub>7</sub> asphaltenes extracted from fresh crude using ASTM D 6560. It is observed that the crude oil before and after use loses appreciable weight (~96%) as the temperature is ramped up from 30 to 475 °C. The nature of crude changes to a small extent. No weight loss was observed in the soft deposit sample up to 160 °C.

The weight loss in soft deposit is ~10.31% and ~83.91% at temperatures up to 300 and 475 °C respectively. This indicates the presence of heavier material in soft deposit which are potentially formed via chemical reactions of precursors transported from the bulk or in the crude sample near the coupon surface. The combustible component in soft deposit is also higher, i.e. ~8.5% as compared to ~2.5% in the crude.

The characterization of hard deposits presented in the preceding sections leads to the conclusion that fouling is corrosion-based at the temperatures and RPMs investigated. This conclusion is in agreement with fouling results reported in past studies [14], [16], [17].

### Proposed Mechanism of fouling

At temperatures greater than 220 °C, naphthenic acid in crude oil leads to the formation of iron naphthenate. The iron naphthenate can directly react with H<sub>2</sub>S to form FeS on the surface. This reaction is however unlikely due to the presence of oxides of iron being detected in the XRD spectra of hard

deposit. Therefore, it is likely that iron naphthenate thermally decomposes into FeO.

FeO is however thermodynamically unstable and forms Fe<sub>2</sub>O<sub>3</sub>/Fe<sub>3</sub>O<sub>4</sub> along with iron (Fe). The Fe then reacts with H<sub>2</sub>S to form FeS. The formation of the sulfide layer promotes further fouling with organic species in the soft deposit increasingly adhering to the FeS or iron oxide layers. The organic content in the hard deposit subsequently increases which then inhibits the formation of FeS and iron oxides.

### CONCLUSIONS

The feasibility and potential of a custom designed coupon test rig has been experimentally demonstrated to study fouling in refinery streams. The test rig facilitates the use of coupon strips of simple geometry instead of the normally adopted tubular and annular surfaces, which greatly enhances the ease of operation during experimentation. The coupons represent differential surface elements of fouling heat transfer surfaces at constant temperature and near uniform shear stress [19]. The test rig enables studies to be made of the effect of varying bulk temperature on foulant deposition and subsequent collection and characterization of deposits using a consistent repeatable and reproducible analytical protocol.

Both bulk temperature and RPM were found to have an effect on the amount of foulant deposited on a coupon. The deposits formed were found to strongly or loosely bound to a coupon surface and are classified as hard and soft deposits respectively.

Studies conducted using a representative refinery stream indicated FeS based corrosion to be the primary cause of fouling at the temperature and RPM levels investigated. The corrosion process is initiated via naphthenic acid attack on a metal surface leading to formation of oxides of iron and subsequently FeS. Organic species from soft deposit adhere to the FeS/iron oxide layer depending on temperature and stream velocity. The increase in organic content in the hard deposit inhibits the corrosion rate. Thus, both hard and soft deposit contribute to the fouling phenomena.

The rig can be used to study and understand relative impact of operating conditions on fouling at temperatures greater than 300 °C which is the scope of future work that includes understanding the contribution of soft deposit to the fouling process and estimate activation energies.

### NOMENCLATURE

$\tau$	shear stress, Pa
$Re$	Reynolds number
$\rho$	fluid density, kg/m <sup>3</sup>
$u$	linear velocity, m/s
$\Omega$	angular velocity, s <sup>-1</sup>
$R_c$	distance between the shaft and coupon surface, 0.017 m

L width of the coupon, 0.012 m  
 $\nu$  kinematic viscosity of the fluid, m<sup>2</sup>/s  
 N rotational speed, RPM

### Subscript

c coupon surface

### REFERENCES

- [1] Watkinson, A. P., Deposition from crude oils in heat exchangers, *Heat Transf. Eng.*, vol. 28, no. 3, pp. 177–184, 2007.
- [2] Ishiyama, E. M., Paterson, W. R., and Wilson, D. I., The effect of fouling on heat transfer, pressure drop, and throughput in refinery preheat trains: Optimization of cleaning schedules, *Heat Transf. Eng.*, vol. 30, no. 10–11, pp. 805–814, 2009.
- [3] Young *et al.*, Characterization of crude oils and their fouling deposits using a batch stirred cell system, *Heat Transf. Eng.*, vol. 32, no. 3–4, pp. 216–227, 2011.
- [4] Fan, Z., Rahimi, P., McGee, R., Wen, Q., and Alem, T., Investigation of fouling mechanisms of a light crude oil using an alcor hot liquid process simulator, *Energy and Fuels*, vol. 24, no. 11, pp. 6110–6118, 2010.
- [5] Crittenden, B. D., Kolaczowski, S. T., Takemoto, T., and Phillips, D. Z., Crude Oil Fouling in a Pilot-Scale Parallel Tube Apparatus, *Heat Transf. Eng.*, vol. 30, no. 10–11, pp. 777–785, 2009.
- [6] Smith, A. D., Analysis Of Fouling Rate And Propensity For Eight Crude Oil Samples In Annular Test Section, *Int. Conf. Heat Exch. Fouling Clean. - 2013*, vol. 2013, pp. 1–8, 2013.
- [7] Rafeen, M. S., Mohamed, M. F., Mamot, M. Z., Manan, N. A., Shafawi, A., and Ramasamy, M., Crude Oil Fouling: PETRONAS Refineries Experience, in *Heat Exchanger Fouling and Cleaning VII*, pp. 8–12, 2007.
- [8] Muñoz Pinto, D. A., Cuervo Camargo, S. M., Orozco Parra, M., Laverde, D., García Vergara, S., and Blanco Pinzon, C., Formation of fouling deposits on a carbon steel surface from Colombian heavy crude oil under preheating conditions, *J. Phys. Conf. Ser.*, vol. 687, no. 1, 2016.
- [9] Srinivasan, M., and Watkinson, A. P., Fouling of some Canadian crude oils, *Heat Transf. Eng.*, vol. 26, no. 1, pp. 7–14, 2005.
- [10] Bennett, C. A., Kistler, R. S., Nangia, K., Al-Ghawas, W., Al-Hajji, N., and Al-Jemaz, A., Observation of an isokinetic temperature and compensation effect for high-temperature crude oil fouling, *Heat Transf. Eng.*, vol. 30, no. 10–11, pp. 794–804, 2009.
- [11] Wang, W., and Watkinson, A. P., Iron sulphide and coke fouling from sour oils: Review and initial experiments, in *Proc. International Conference on Heat Exchanger Fouling and Cleaning IX*, pp. 23–30, 2011.
- [12] Saleh, Z. S., Sheikholeslami, R., and Watkinson, A. P., Fouling characteristics of a light Australian crude oil, *Heat Transf. Eng.*, vol. 26, no. 1, pp. 15–22, 2005.
- [13] Diaz-Bejarano, E., Behranvand, E., Coletti, F., Mozdianfard, M. R., and Macchietto, S., Organic and Inorganic Fouling in Heat Exchangers-Industrial Case Study: Analysis of Fouling Rate, *Ind. Eng*
- [14] Behranvand, E., Mozdianfard, M. R., Diaz-Bejarano, E., Coletti, F., Orzowski, P., and Macchietto, S., A comprehensive investigation of refinery preheaters foulant samples originated by heavy crude oil fractions as heating fluids, *Fuel*, vol. 224, pp. 529–536, 2018.
- [15] Shank, R. A., and McCartney, T. R., Characterization of crude oil fouling: Defining the coke spectrum, in *Heat Exchanger Fouling and Cleaning*, 2019.
- [16] Wang, W., and Watkinson, A. P., Deposition from a sour heavy oil under incipient coking conditions: Effect of surface materials and temperature, *Heat Transf. Eng.*, vol. 36, pp. 623–631, 2015.
- [17] Wang, W., and Watkinson, A. P., Deposition From a Sour Heavy Oil Under Incipient Coking Conditions: Wall Shear Effects and Mechanism, *Proc. Int. Conf. Heat Exch. Fouling Clean.*, vol. 2015, pp. 65–73, 2015.
- [18] Singh P., Krishnaswamy S., Ponnani K., Verma A., and Rawat J., Crude Oil Foulant Deposition Studies on a Heated Surface Using a Novel Batch Stirred Coupon Test Rig, *Int. J. Chem. Eng.*, vol. 2022, pp. 1–10, 2022.
- [19] Ramchandran, P., Sundar, R., Michael, G., and Jovancevic, V., Shear Stress Profile in a Rotating Cage, in *International Conference on Corrosion CORCON*, pp. 26–28, 2007.
- [20] Epstein, N., A Model of the Initial Chemical Reaction Fouling rate for Flow within a Heated Tube and its Verification, in *10th international Heat Transfer Conference*, pp. 225–229, 1994.